J. Korean Wood Sci. & Tech. 41(5) : 456~465, 2013 http://dx.doi.org/DOI : 10.5658/WOOD.2013.41.5.456

Effect of Alternating Vacuum and Release Process on Drying Characteristics of Log Cross Section during Radio Frequency Drying*1

Dan Xie*2, Nam-Ho Lee*3, Yoon-Seong Chang*4, and Hwanmyeong Yeo*4,5 †

ABSTRACT

Log cross sections of yellow poplar were dried in a radio frequency vacuum (RFV) dryer under alternating vacuum and release (AVR) process. The average moisture content (MC), temperature and vapor pressure at the volumetric center were monitored as functions of time. Three different log thicknesses (33, 60 and 75mm) were tested. The results show that the AVR process caused an increase in the drying rate when the moisture content was above fiber saturation point (FSP, about 30% MC) but that it had an inverse effect on the drying rate when the MC was below FSP. The effect of the AVR process on the drying rate decreased, and the severity of heart checks increased, with the increase in the thickness of the specimens.

Keywords : alternating vacuum and release (AVR) process, radio frequency vacuum drying (RFV), electromagnetic field, drying rate, temperature, moisture content, vapor pressure

1. INTRODUCTION

The radio frequency vacuum (RFV) drying technology is a method that constitutes a combination of rapid heating by a high-frequency current and a rapid drying rate in a vacuum, where the boiling temperature of water is decreased with decreasing pressure. When a green piece of wood is placed which in a high-frequency alternating electromagnetic (EM) field, the water dipoles and the ions located in the lumens and cell walls oscillate according to the direction of the EM field. As a result, the heat from the molecular friction of the water molecules in the wood is generated within the wood. The intensity of the heating directly depends on the

*1 Received on August 22, 2013; accepted on September 24, 2013
*2 (Former) Department of Wood Science & Technology (Institute of Agricultural Sci. & Tech.), Chonbuk National University, 567 Baekje-daero, deokjin-gu, Jeonju, 561-756, Republic of Korea
*3 Department of Wood Science & Technology (Institute of Agricultural Sci. & Tech.), Chonbuk National University, 567 Baekje-daero, deokjin-gu, Jeonju, 561-756, Republic of Korea
*4 Department of Forest Sciences, College of Agriculture and Life Sciences, Seoul National University, 1 Gwanak-ro, Gwanak-gu, Seoul, 151-921, Republic of Korea
*5 Research Institute for Agriculture and Life Sciences, College of Agriculture and Life Sciences, Seoul National University, 1 Gwanak-ro, Gwanak-gu, Seoul, 151-921, Republic of Korea
† Corresponding author : Hwanmyeong Yeo (e-mail: hyeo@snu.ac.kr)

electric field and on the average moisture content (MC) of the wood. Furthermore, high temperatures are not required for vaporization and moisture removal due to the vacuum (Leiker and Adamska, 2004). Therefore, a rapid drying rate, lower internal drying stresses, a uniform final MC distribution, and reduced defects are the obvious advantages of the RFV drying technology when compared to the conventional kiln drying technology (Harris and Taras, 1984; Avramidis and Zwick, 1996).

Some studies were carried out to investigate the moisture content, temperature and vapor pressure distribution within wood to understand the mechanism of RFV drying. Generally, during RFV drying, the temperatures within wood were quite uniform except near the end of the specimen (Zhang *et al.*, 1997), and the pressure difference (△p) between the internal pressure of wood and the ambient pressure played a big role on drying force during RFV drying (Cai and Hayashi, 2001). Avramidis *et al.* (1994) reported that temperature and vapor pressure gradients developed in the longitudinal direction of board and contributed to the high drying rates during drying of thick western redcedar. Liu *et al.* (1994) also reported that the pressure difference between the middle section and the end surface was the drying force for moisture transfer, and the increase of pressure gradients resulted in shorter drying times. △p between the continuous internal water evaporation and the external vacuum is the most obvious internal mass transport mechanism above FSP (Koumoutsakos *et al.*, 2001a). But the △p, which the drying force, decreased during drying process (Liu *et al.*, 1994; Koumoutsakos *et al.*, 2001b).

Thus, the hypothesis that the increased △p between the internal vapor pressure of wood and the ambient pressure will result in an increase in the drying rates was supported. In this study, alternating vacuum and release (AVR) process was used to increase the internal vapor pressure of wood.

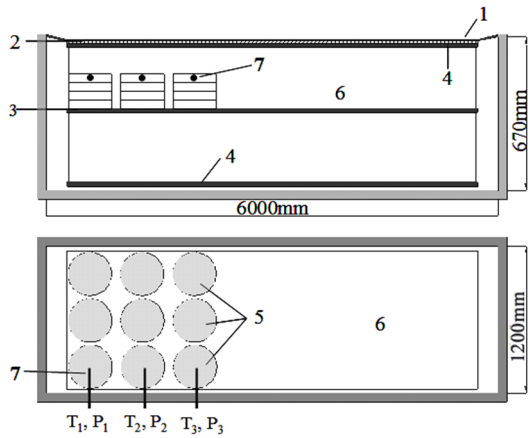

1: rubber sheet 2: insulation plate
3: charge plate 4: ground plate
5: specimens 6: dummy log cross-sections
7: temperature and pressure probe
T: Temperature
P: Pressure

Fig. 1. Schematic of the RFV dryer and stacking of 33-mm-thick log cross-sections.

The aim of this study was to investigate the effect of the AVR process on the drying characteristics (e.g., MC, drying rate, temperature, vapor pressure and final quality) of the Yellow poplar log cross-section, which has been used as a raw material for wood carving and interior product, during RFV drying.

2. MATERIALS and METHODS

2.1. Radio Frequency Vacuum Dryer

The internal dimensions of the chamber that was connected to RF heating were a length of 6,000 mm, a width of 1,200 mm, and a height of 670 mm (Fig. 1). The frequency was set at approximately 13 MHz, and the maximum output of the RF generator was 25 kW. The generator was operated in an 8-min-on - 2-min-off cycle. The center electrode plate, which was

Table 1. Numbers, diameter, and average initial MC of the yellow-poplar log cross-sections

Species		Numbers of Specimens (pieces)			Initial Moisture Content (%)		
Thickness (mm)	Diameter (mm)	V_{10}-R_0	V_{10}-R_1	V_{10}-R_2	V_{10}-R_0	V_{10}-R_1	V_{10}-R_2
33	200~220	36	36	36	77.6	78.5	77.4
60	310~340	9	0	9	111.7	-	109.8
75	310~340	9	0	9	112.4	-	117.1

connected to the RF generator, was positive while the top and bottom plates, which were grounded to the chamber, were negative. The ambient pressure in the chamber was controlled by a liquid ring vacuum pump, and the ambient pressure was maintained at 0.10 atm.

2.2. Experimental Procedure

Yellow poplar log cross sections were cut from green logs with a length of 1.8 m and the average diameter of 210 mm. The numbers, diameter and average initial MC of log cross sections that were used in this study are shown in Table 1. All the specimens were dried in a vacuum for 10 hr and then released in ambient air. After 2 hr, the specimens were put into the chamber to dry again. After 10 hr vacuum drying, the specimens were taken out from chamber and released in ambient air for 2 hr. This method, which the specimens were dried by alternating vacuum and release process, named AVR process. The specimens were dried with AVR process until the end of drying. To investigate the effect of the release time on the increase in the vapor pressure, the log cross-section in the 33-mm group were dried using three release times (0 hr, 1 hr, 2 hr), named V_{10}-R_0, V_{10}-R_1 and V_{10}-R_2 processes, respectively. During the release process, the V_{10}-R_0 processspecimens were placed inside enclosed plastic bags for 2 hr, and the V_{10}-R_1 process specimens were placed inside enclosed plastic bags for 1 hr. The V_{10}-R_2 process specimens were released in ambient air for 2 hr.

The temperature and internal vapor pressure of the volumetric center of the log cross-sections were monitored simultaneously by fiber-optic sensor. All the process data were collected at 30 sec and were saved in a PC using a data acquisition system. Specimens were solid-stacked between the electrode plates. The MC was calculated using the weight of specimens measured during the drying as well as the weight of oven-dried specimens (T = 103 ± 2°C t = 24 h). After drying, the numbers and length of heart checks, border checks and V-cracks on the end surface of the specimens were visually evaluated.

3. RESULTS and DISCUSSION

3.1. Drying Curve and Rate

Fig. 2 plots the average MC-time curves of the 33-mm-, 60-mm-, and 75-mm-thick log cross section when the AVR process was used. In the 33-mm group, the total drying times were the same for the three processes (Table 2). It can be seen, though, that the average drying rate of the V_{10}-R_2 process became the highest at 95 hr (Fig. 2). It is also interested to note that the drying time when the MC of the V_{10}-R_2 process reached 30% was 98 hr (Table 2). The average drying rate of the V_{10}-R_2 process was

Table 2. Drying time and average drying rate during the RF/V drying of the 33-mm-thick yellow-poplar log cross-section

Species		Drying Time (hr)			Drying Rate (%/hr)		
Thickness (mm)	Process	Green~11%	Green~30%	30%~11%	Green~11%	Green~30%	30%~11%
33	V_{10}-R_0	121	98	23	0.550	0.486	0.826
	V_{10}-R_1	122	91.4	30.6	0.553	0.531	0.621
	V_{10}-R_2	122	87.8	34.2	0.544	0.540	0.555

Note : (a) The drying time and drying rate were corrected by interpolation or extrapolation.

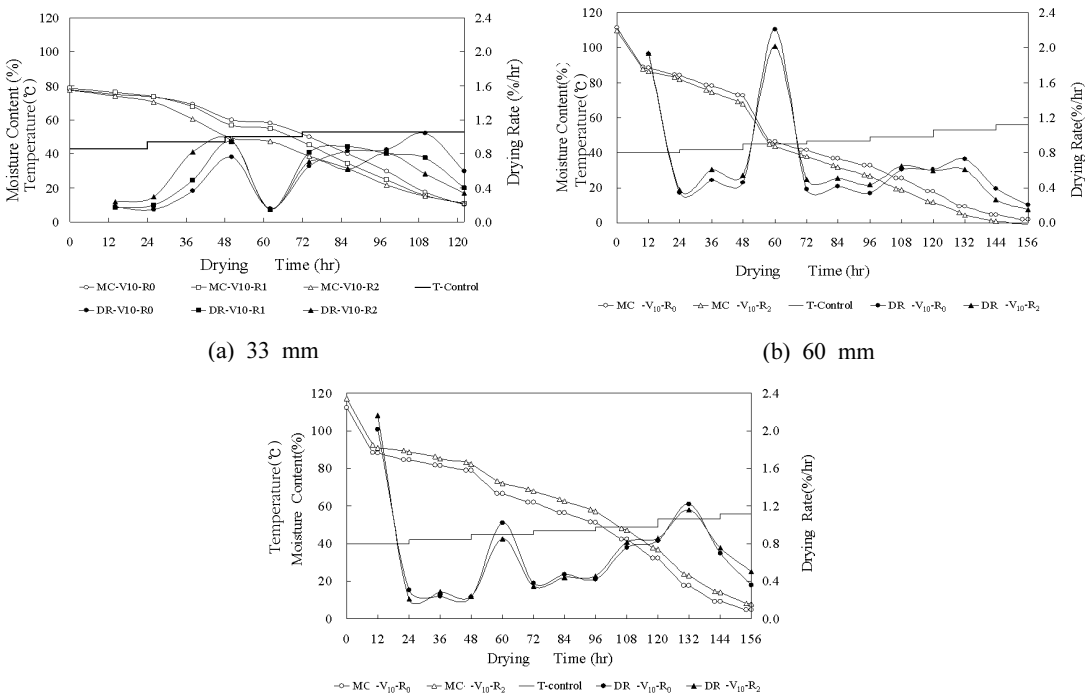

(a) 33 mm

(b) 60 mm

(c) 75 mm

Fig. 2. MC-time and drying rate (DR) curves during the RF/V drying of the 33-mm-, 60-mm-, and 75-mm-thick yellow-poplar log cross-section (MC: Moisture content, DR: Drying rate).

the highest, and that of the V_{10}-R_1 process when the MC decreased from green to 30% was higher than that of V_{10}-R_0 process (0.486, 0.531, 0.540 %/hr for the V_{10}-R_0, V_{10}-R_1 and V_{10}-R_2 process, respectively). The average drying rate of the V_{10}-R_2 process became the lowest, however, when the MC loss was from 30% to 11% (0.826, 0.621, and 0.555 %/hr for the V_{10}-R_0,

Table 3. Drying time and average drying rate during the RF/V drying of the 60-mm- and 75-mm-thick yellow-poplar log cross-section

Species		Drying Time (hr)			Drying Rate (%/hr)		
Thickness (mm)	Process	Green~10%	Green~30%	30%~10%	Green~10%	Green~30%	30%~10%
60	V_{10}-R_0	131.0	100.4	30.6	0.776	0.813	0.654
	V_{10}-R_2	122.8	88.2	34.6	0.813	0.905	0.578
75	V_{10}-R_0	143.0	121.9	21.1	0.716	0.676	0.947
	V_{10}-R_2	152.1	126.0	26.0	0.704	0.691	0.769

Note : (a) The drying time and drying rate were corrected by interpolation or extrapolation.

V_{10}-R_1 and V_{10}-R_2 process, respectively). In the 60-mm group, the increase in the average drying rate from 0.776 %/hr to 0.813 %/hr can be seen in Table 3. The average drying rate of the V_{10}-R_2 process was higher than that of the V_{10}-R_0 process before 120 hr, but became lower than that of the V_{10}-R_0 process after 120 hr (Fig. 2). Table 3 also shows that the average drying rate of V_{10}-R_2 process was higher than that of the V_{10}-R_0 process when the MC loss was from green to 30% (0.813 and 0.905 %/hr for the V_{10}-R_0 and V_{10}-R_2 process, respectively), but was lower than that of the V_{10}-R_0 process below 30% (0.654 and 0.578 %/hr for V_{10}-R_0 and V_{10}-R_2 process, respectively).

In the 75-mm group, the increase in the drying rate of the V_{10}-R_2 process before 30% can be seen in Table 3, but it became lower than that of the V_{10}-R_0 process when the MC was from 30% to 10%. These results show that the drying rate increased, as s result of the use of the AVR process, when the MC was from green to 30%, but decreased when the MC was below 30%. This difference is presumably the result of different mechanisms of internal mass transfer. If 30% is considered the FSP, when the MC is above it, the continuous internal water evaporation and the external vacuum make the vapor bulk flow due to pressure gradients, the most obvious internal mass transport mechanism above FSP. Below FSP, the bound water diffusion can be considered the predominant mass transfer mechanism. The main effects of pressure on mass transfer are worth noting and should be studied further (Koumoutsakos *et al.*, 2003 Perre *et al.*, 2004).

3.2. Temperature and Pressure Profiles

Fig. 3 depicts the internal temperature profile (volumetric center of the specimens) with time in the 33-mm, 60-mm, and 75-mm-thick log cross sections when the AVR process was used. At the beginning of the drying process, the temperatures increased because most of the heat that was generated within the wood was consumed for heating. In the course of the drying process, the temperatures remained constant and followed similar patterns. There was a considerable increase in temperature, however, at the end of the drying process.

In the 33-mm group, the temperature in the V_{10}-R_2 process was lower than that in the other process from 24 hr to 98 hr. In the 60-mm and 75-mm groups, the temperature in the V_{10}-R_2 process was lower than that in the V_{10}-R_0 proc-

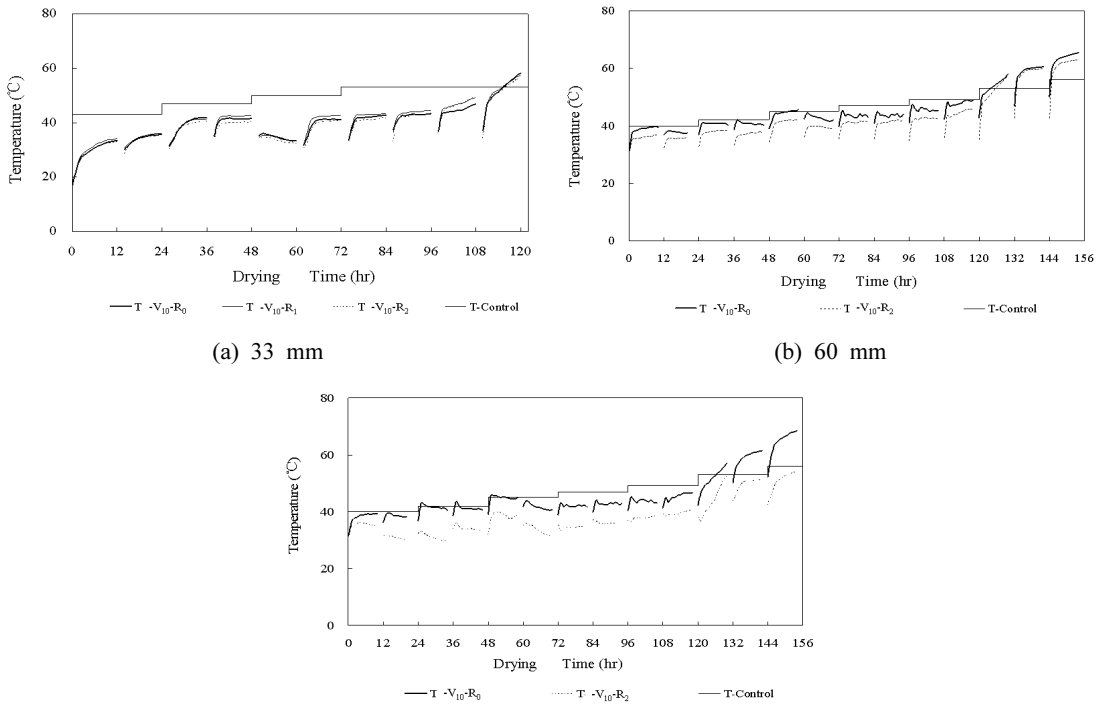

(a) 33 mm (b) 60 mm

(c) 75 mm

Fig. 3. Temperature variations with time during the RF/V drying of the 33-mm-, 60-mm-, and 75-mm-thick yellow-poplar log cross-section (T: Temperature of wood).

ess during the entire drying process. This can be attributed to the quick removal of moisture. The heat that was generated within the wood was consumed for evaporation purposes. These results coincided with the average drying rate, that is, the average drying rate of the V_{10}-R_2 process was lower than that of the other processes at this time. The decrease in the dielectric loss factor (Torgovnikov, 1993) explains why the average drying rate decreased at the end of the drying process, although the temperature increased significantly (Fig. 3).

Fig. 4 describes the internal vapor pressure variations as a function of time in the 33-mm-, 60-mm- and 75-mm-thick log cross sections, respectively. The internal vapor pressure was not smooth at every AVR cycle. It exhibited an initial drop when the vacuum pump started. Due to the evaporation of water resulting from the volumetric heating, an increase in vapor pressure was observed after this initial reduction. It was noticed that the vapor pressure in the V_{10}-R_0 process was lower than that in the AVR process (the vapor pressure in the V_{10}-R_0 process in the 75-mm group was not obtained because a problem was encountered with the pressure sensor). It can be said that the empty lumen cells were full of air due to the pressure difference between the ambient air and the internal pressure of the specimens when released in ambient air. No further increase in vapor pressure was observed, however, as the release

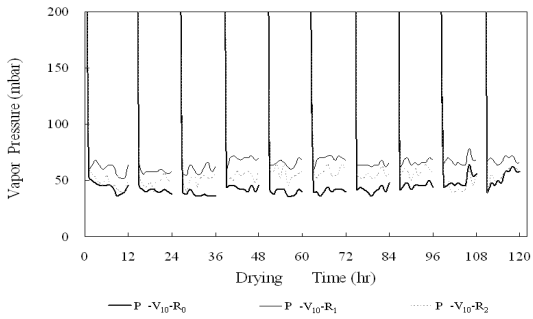

(a) 33 mm

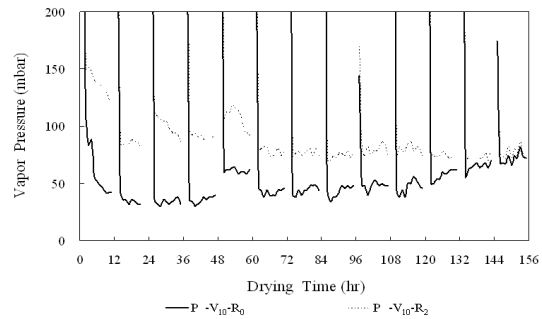

(b) 60 mm

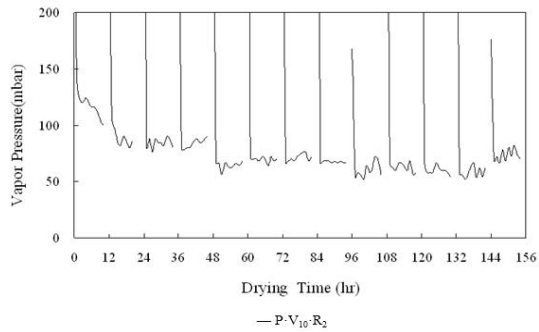

(c) 75 mm

Fig. 4. Pressure variations with time during the RF/V drying of the 33-mm-, 60-mm-, and 75-mm-thick yellow-poplar log cross-section (P : Vapor pressure of wood).

time was increased. The vapor pressure in the V_{10}-R_1 process was higher than that in the V_{10}-R_2 process (Fig. 4: 33 mm). Moreover, the internal vapor pressure in the AVR process did not decrease or increased very slowly during the drying process. This coincides with the hypothesis that the AVR process will increase the vapor pressure, resulting in anincrease in the drying rate.

Fig. 5 shows the pressure and the temperature in specimen increased during the RFV drying of the 33-mm-thick log cross section, where Ts is the boiling point corresponding to the internal vapor pressure. The temperatures in the specimens quickly increased and became higher than Ts. Therefore, free water was boiling when the temperature reached Ts. This indicates that moisture transport and removal occurs mainly in the vapor form.

3.3. Checks of Dried Log Cross Section

Table 4 contains a summary of the data obtained for heart checks, border checks and V-cracks after RFV drying. There were no checks during the 33-mm AVR process drying. No heart check occurred during the V_{10}-R_2 drying process in the 60-mm group due to the quick removal of the MC. The heart checks resulting from the large tangential expansion and radial contraction under heat were significantly reduced by the driving force of free water de

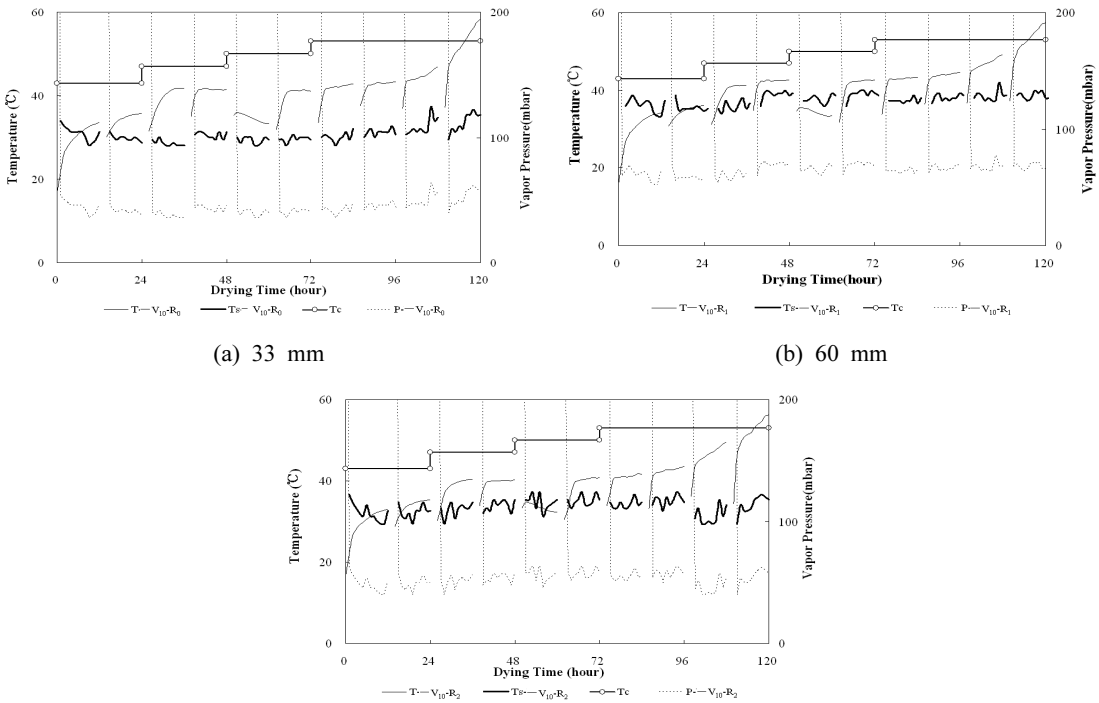

(a) 33 mm

(b) 60 mm

(c) 75 mm

Fig. 5. The process of pressure and temperature increase in the specimens during the RF/V drying of the 33-mm-, 60-mm-, and 75-mm-thick yellow-poplar log cross-section (T: Temperature of wood, Ts : Boiling point corresponding to internal vapor pressure of wood, Tc : Control temperature according to drying schedule, P : Vapor pressure of wood).

Table 4. Percentage of disks that incurred defects due to heart checks, and average number and length/width of heart checks and V-cracks per disk

Species		Heart Check		Border Check			V- Crack			Sound
Thickness (mm)	Process	Percentage of defected disk (%)	Length (mm)	Percentage of defected disk (%)	Length (mm)	Location	Percentage of defected disk (%)	Length (mm)	Width (mm)	Percentage of sound disk (%)
33	V_{10}-R_0	0	0	0	0	0	0	0	0	100
	V_{10}-R_1	0	0	0	0	0	0	0	0	100
	V_{10}-R_2	0	0	0	0	0	0	0	0	100
60	V_{10}-R_0	11	3.5	67	355.0	0.46	67	109.5	6.9	11
	V_{10}-R_2	0	0	82	248.9	0.55	82	113.7	12.9	9
75	V_{10}-R_0	40	59.5	100	437.6	0.62	100	221.9	24.8	0
	V_{10}-R_2	67	103.1	100	673.6	0.64	100	254.6	23.8	0

veloped inherently in an RFV kiln (Lee *et al.*, 1998). Therefore, the AVR process was shown to be capable of preventing heart checks in the 60-mm group. Nevertheless, the V_{10}-R_2 process specimens showed severe defects in the 60- and 75-mm groups. A reduction of the increase in the drying rate and in the severity of checks resulting from the AVR process was observed with the increase in the thickness of specimens (Fig. 2, Table 4).

4. CONCLUSION

The AVR process increased the internal vapor pressure of the volumetric center of the log cross-sections, which resulted in an increase in the drying rate above FSP and a decrease in the drying rate below FSP. The increase in the internal vapor pressure was not proportional to the release time. The effect of the AVR process on the drying rate decreased, and the severity of heart checks increased, with the increase in the thickness of the specimens. It can thus be concluded that the AVR process can be used to increase the drying rate above FSP, without producing defects, during RFV drying of thin and yellow-poplar log cross-section.

ACKNOWLEDGMENT

This study was carried out with the support of Forest Science & Technology Projects.

REFERENCES

1. Avramidis, S., F. Liu, and B. J. Neilson. 1994. Radio-frequency/vacuum drying of softwoods: drying of thick western red cedar with constant electrode voltage. Forest Products Journal 44(1): 41~47.
2. Avramidis, S. and R. L. Zwick. 1996. Commercial-scale RF/V drying of softwood lumber. Part 2. Drying characteristics and lumber quality. Forest Products Journal 46(6): 27~36.
3. Cai, Y. and K. Hayashi. 2001. Pressure and temperature distribution in wood during radio-frequency/vacuum drying. In: The seventh international IUFRO wood drying conference, Tsukuba, Japan, pp. 386~391.
4. Harris, R. A. and M. A. Taras. 1984. Comparison of moisture content distribution, stress distribution and shrinkage of red oak lumber dried by a radio-frequency/vacuum drying process and a conventional kiln. Forest Products Journal 34(1): 44~54.
5. Koumoutsakos, A., S. Avramidis, and S. G. Hatzikiriakos. 2001a. Radio frequency vacuum drying of wood. I: Mathematical model. Drying Technology 19(1): 65~84.
6. Koumoutsakos, A., S. Avramidis, and S. G. Hatzikiriakos. 2001b. Radio frequency vacuum drying of wood. II: Experimental model evaluation. Drying Technology 19(1): 85~98.
7. Koumoutsakos, A., S. Avramidis, and S. G. Hatzikiriakos. 2003. Radio frequency vacuum drying of wood. III: Two-dimensional model, optimization, and validation. Drying Technology 21(8): 1399~1410.
8. Lee, N. H., K. Hayashi, and H. S. Jung. 1998. Effects of radio-frequency/vacuum drying and mechanical press-drying on shrinkage and checking of walnut log cross section. Forest Technology 48(5): 73~79.
9. Leiker, M. and M. A. Adamska. 2004. Energy efficiency and drying rates during vacuum microwave drying of wood. European Journal of Wood and Wood Products 62: 203~208.
10. Liu, F., S. Avramidis, and R. L. Zwick. 1994. Drying of western hemlock in a laboratory radio-frequency/vacuum dryer with constant and variable electrode voltage. Forest Products Journal 44(6): 71~75.
11. Perre, P., S. Mosnier, and I. W. Turner. 2004. Vacuum drying of wood with radiative I. Experimental procedure. AIChE J. 50(1): 97~107.
12. Torgovnikov, G. I. 1993. Dielectric Properties of

Wood and Wood‐Based Materials; Springer-Verlag: Berlin, Germany.
13. Zhang, L., S. Avramidis, and G. Hatzikiriakos. 1997. Moisture flow characteristics during radio frequency vacuum drying of thick lumber. Wood Science and Technology 31: 265~277.